View metadata, citation and similar papers at core.ac.uk

brought to you by CORE

provided by Diposit Digital de la Universitat de Barcelona

Elsevier Editorial System(tm) for Ceramics International

Manuscript Draft

Manuscript Number: CERI-D-16-03453R1

Title: Magnesium Phosphate Cement formulated with Low Grade Magnesium Oxide with controlled porosity and low thermal conductivity as a function of admixture

Article Type: Full length article

Keywords: Insulation; building material; design of experiments; MPC; porosity; thermal conductivity

Corresponding Author: Dr. Joan Formosa,

Corresponding Author's Institution:

First Author: Maria Niubó, PhD

Order of Authors: Maria Niubó, PhD; Joan Formosa; Alex Maldonado, PhD student; Ricardo del Valle, PhD; Josep M Chimenos, Associate Professor

Abstract: Magnesium phosphate cement (MPC) formulated with low-grade magnesium oxide (LG-MgO) can be better considered as sustainable MPC (sust-MPC). Among other properties, sust-MPC could be used as building material for constructive elements because of its acoustic and thermal insulation properties. Porosity and thermal conductivity are two important parameters that have a significant influence on thermal insulation properties. In this regard, this work aimed to obtain a highly porous sust-MPC with enhanced properties for thermal insulation. To this end the percentage of porosity as a function of both the amount of set-retarding admixture and the kneading water needed was assessed using a statistical design of experiments (DoE) approach. Additionally, thermal conductivity was also evaluated with respect these two factors. Last but not least, an optimized dosage was sought in order to maximize the percentage of porosity while achieving the lowest thermal conductivity. According to the results obtained, the statistical method successfully predicted the effects of variables on the final properties. Hence, a model that explains the overall behaviour of the system was successfully attained. The obtained model predicts the porosity and the thermal conductivity of sust-MPC by means of the mixture dosage. Consequently, the present work demonstrates that it is possible to control the porosity in order to diminish thermal conductivity.

Response from the authors:

The authors would like to thank the editor and the reviewer for their valuable comments. According to the editor's comments:

Reviewer #1:

Reviewer #1: The paper presents a study about magnesium phosphate cement formulated with low grade magnesium oxide. The paper shows relation between thermal conductivity, mechanical properties, open porosity with the water to binder ratio and the amount of retardant. The experimental part is well conducted, we may regret that the paper is only based on experimental results and does not explain in more detail the relationship between properties and microstructure.

First of all, we would like to acknowledge your kind recommendations.

Page 5 lines 48-51: *Reviewer's comment*: "*the term mortar should be resricted to a mix with defined particle size (sand 0-4mm and cement). It is not the case here, I would prefer to avoid the term mortar here*".

Response: The MPC developed with LG-MgO could be considered as a mortar instead of a cement paste due the inert phases (carbonates, SiO_2, etc.) that remaining in the material. Then, we consider these kind of MPCs as mortars instead of cement pastes. In addition we would like to emphasize that this is the most important factor among others researchers groups in this topic. Please, we would be grateful if you reconsider this matter.

You can please check the reference [38] for further information on this matter.

Page 6 line 27: *Reviewer's comment*: "*The mixing protocol is certainly very important and should be described in details here".*

Response: We agree. On this manner, we included the description of the mixing procedure, although in the section 2.3.

"The mixing procedure was conducted as follows: MKP, LG-MgO and boric acid were weighed, respectively, and putted into a jar and carefully mixed in a dry state by hand operation using a spoon for 2 minutes. Afterwards, the kneading water was added and the mixing was conducted by a commonly planetary mortar mixer during 120 seconds at slow speed and 60 seconds at fast speed."

Page 6 line 39: *Reviewer's comment* "*add a reference*"

Response: We added the reference.

Page 9 lines 24-27: *Reviewer's comment* "*may be justified the choice of 14 days, do we have any variation of the properties after? Do we have a stabilization of the mass at 14 days?..."*

Response: We would like to emphasize that we conducted the experiments after 28 days. Please, you may revise the manuscript document, section 2.4., before the beginning of section 2.4.1. "*All the experiments were carried out at 28 days (14 days of curing and 14 days of drying)*."

We studied the properties after 28 days, 14 days of curing and 14 days of drying. So, the main purpose was to evaluate the properties at 28 days and before that we need to dry the samples for the tests. On this manner, we concluded that it was necessary a minimum period of time of 10 days by using silica gel methodology. Then, we decide to cure and to dry during the same period of time just to conduct the experiments at 28 days of the specimens' life.

Page 13 line 52: *Reviewer's comment:* "*a link with permeability and a study using MIP may be interesting in the future. Do we have any information about porosity not accessible?*"

Response: We agree. This is an important study to be considered for further studies. Although, currently we do not have information about not accessible, we will consider this for the on-going research. We appreciate so much this observation.

Page 20 lines 47-53: *Reviewer's comment "same"*

Response: Thank you very much for this comment. We corrected the reference.

*Manuscript
Click here to view linked References

Magnesium Phosphate Cement formulated with Low Grade Magnesium Oxide with controlled porosity and low thermal conductivity as a function of admixture

M. Niubó[1], J. Formosa[1*], A. Maldonado-Alameda[1], R. del Valle-Zermeño[1], J.M. Chimenos[1]

[1]Departament de Ciència de Materials i Química Física. Ciència i Enginyeria de Materials, Universitat de Barcelona, Martí i Franquès 1, 08028 Barcelona, Spain.

*Author to who correspondence should be addressed. Telephone: +34934021316; Fax: +34934035438; E-mail: joanformosa@ub.edu

Abstract

Magnesium phosphate cement (MPC) formulated with low-grade magnesium oxide (LG-MgO) can be better considered as sustainable MPC (sust-MPC). Among other properties, sust-MPC could be used as building material for constructive elements because of its acoustic and thermal insulation properties. Porosity and thermal conductivity are two important parameters that have a significant influence on thermal insulation properties. In this regard, this work aimed to obtain a highly porous sust-MPC with enhanced properties for thermal insulation. To this end the percentage of porosity as a function of both the amount of set-retarding admixture and the kneading water needed was assessed using a statistical design of experiments (DoE) approach. Additionally, thermal conductivity was also evaluated with respect these two factors.

Last but not least, an optimized dosage was sought in order to maximize the percentage of porosity while achieving the lowest thermal conductivity. According to the results obtained, the statistical method successfully predicted the effects of variables on the final properties. Hence, a model that explains the overall behaviour of the system was successfully attained. The obtained model predicts the porosity and the thermal conductivity of sust-MPC by means of the mixture dosage. Consequently, the present work demonstrates that it is possible to control the porosity in order to diminish thermal conductivity.

1. Introduction

Overall, porosity has an important role in the mechanical properties of concrete, cement and ceramic composites. A reduction of porosity increases the materials strength, particularly in cement based composites [1,2]. This parameter has also influence on the durability of the cement material. The influence of porosity on compressive and tensile strength was already studied by X. Chen et al. [3] which conclude that the effects of porosity are not constant. Nevertheless, a higher porosity leads to a better acoustic and thermal insulation. In recent years, in several countries of mild climate, more attention has been given to reducing energy consumption whilst maintaining or improving comfort conditions in buildings.

The thermal conductivity of building materials is an increasingly important parameter that significantly influences the energy associated with heating and cooling in buildings. For improving thermal conductivity, the addition of many different fillers on cement based materials have been reported, including cellulose and glass fibre, mineral wool, polystyrene, urethane foam and vermiculite [4][5]. However, attaining a good dimensional stability and using industrial by-products for increasing resource efficiency

have been scarcely reported. In this regard, relevant researches have included works on lightweight cement-based materials containing waste glass, fly ash, silica fume, tyre rubber, expanded clay, wood and paper [6–8].

The effective thermal conductivity of a ceramic material is strongly affected by its chemical composition as well as by the porosity present in the microstructure. The presence of voids, the distribution and interconnectivity of pores, and the nominal composition are all likely to play roles in determining the effective thermal conductivity [9]. Dos Santos found that moisture and porosity dramatically affects thermal properties of conventional refractory concrete [10]. As higher the material porosity the influence of the water increases, since larger water content can be kept inside the structure. On the other hand, the same author also concluded that thermal conductivity of concrete increases as moisture content increases. Since water has about 25 times higher conductivity than air, it is clear that when the air in the pores has been partially displaced by water or moisture, the concrete increases its thermal conductivity [11,12]. Steiger and Hurd [13] reported a relationship between the gain weight due to water absorption and thermal conductivity: increasing 1% unit weight entails a 5% increase in thermal conductivity.

Concrete's thermal conductivity increases along the cement content [14] and the thermal characteristics of aggregate [15]. Silica fume causes a decrease in the thermal conductivity and an increase in the specific heat of mortar [16].

Ordinary Portland Cement (OPC) is the most widely used hydraulic cement in the world, because it covers a wide range of properties and possibilities. Besides, OPC is an inexpensive material. However, in recent years other more specific types of cements have been developed, which are able to extend the range of work and their applications in other fields of technology. These types of newly developed cements include those

known as chemically bonded ceramics (CBCs) [17]. CBCs are ceramic materials that possess certain characteristics of cement and thus can be considered as such. In general, CBCs are obtained from the acid–base chemical reaction into an aqueous phase between a metal cation and an oxoanion source. When phosphates are used as oxoanion raw material, the CBC becomes chemically bonded phosphate ceramic (CBPC). These CBPCs are normally used as stabilizing agents [18] and/or for the encapsulation of hazardous substances with a high potential for leaching [19,20]. Moreover, CBPC presents very fast setting time and good mechanical properties; for this reason CBPCs can also be used as materials for the quick repair of concrete structures.

The formation of CBPC is controlled by the dissolution and hydrolysis of metal oxides. Hence, the reactivity of the metal oxide is a main factor for the correct formation of these cements [21,22]. It is possible to use MgO and KH_2PO_4 for the formation of one of the CBPCs with best properties [22], struvite-K - $KMg(PO_4)\cdot 6H_2O$ - [23]. Concretely, these cements are commonly named Magnesium Phosphate Cement (MPC) [24–34].

During the last years the authors have reported very promising results of a new MPC developed with Low-Grade Magnesium Oxide (LG-MgO) by-products. By this manner, the cost of the MPC could be sustainable diminished while enhancing sustainable criteria and recyclability. Moreover, previous works carried out by the research group demonstrated that some inert phases form the by-product, such as carbonates and quartz, remained in MPC [35,36]. Accordingly, the MPC developed with LG-MgO could be considered as a mortar instead of cement. Taking into account the abovementioned, the MPC formulated with LG-MgO can be better considered as sustainable MPC (sust-MPC) in order to make a distinction from common MPCs.

The main purpose of this study is based on the research group previous experience in obtaining sust-MPC [35–39]. Nowadays, the sust-MPCs obtained has been considered as construction repairing materials [38]. However, sust-MPC could be also considered for acoustic and thermal insulation accordingly with the abovementioned. In this regard, the aim of this research work was to obtain a highly porous sust-MPC with enhanced properties for thermal insulation. In order to follow up this objective, the next parameters were evaluated by using a statistical design of experiments (DoE): the percentage of porosity was assessed as a function of both the amount of retardant additive and the kneading water needed. In this point, it should be emphasized that the exothermic chemical reaction during MPCs formation is related with the porosity of the final products because of the release of water [40]. Likewise, the thermal conductivity was also evaluated with respect these two factors. Last but not least, an optimized dosage was sought in order to maximize the percentage of porosity while obtaining the lowest thermal conductivity.

It should be noted that the present work aimed to diminish thermal conductivity by means of controlling the porosity in the dosage range under study. Besides, this work is the starting point for further modifying the thermal properties of sust-MPC by impregnating paraffins for thermal energy storage (TES). By this manner, thermal comfort inside buildings could be improved while reducing energy consumption [41,42]. Taking this into account, obtaining a model for controlling porosity is a mandatory step prior developing enhanced MPC for TES. Therefore, this study is aimed at establishing a reference for developing sust-MPC for TES, which, to the knowledge of the authors, has never been published before.

2. Experimental procedure

2.1 Materials

Low-grade magnesium oxide (LG-MgO) was supplied by Magnesitas Navarras S.A. located in Navarra (Spain). This LG-MgO is derived from the calcination of natural magnesite in a rotary kiln at 1100 ºC. It is a by-product collected as cyclone dust in the fabric filters from the air pollution control system. Around 100 kg of LG-MgO were taken from various stockpiles.

The source of phosphate employed for this study was monopotassium phosphate (MKP), KH_2PO_4, food grade, which is commonly used as a fertilizer. Moreover, a boric acid, Optibor® technical grade (HB), H_3BO_3, supplied by Borax España, S.A. (Castellón, Spain), was used as a setting time retardant. An exhaustive description of the raw materials was carried out in an earlier study [36] and therefore the present paper only shows significant and relevant information.

2.2 Design of experiments (DoE)

The effect of filler addition on the blend has been usually analysed individually, by a "trial and error" approach. To develop this study a design of experiments was carried out with Design Expert® software [43]. The DoE technique allows for verifying whether or not there is a synergistic effect between the variables on the final properties of the composite or the parameters affecting its manufacturing [44,45]. The main objective of the DoE in this study was to deduce which components influence in major extent the porosity and thermal properties of the sust-MPC formulations. The objective was to quantify the results according to the admixture and therefore its effect over thermal conductivity. On this manner, it could be obtained the desirable thermal conductivity by varying the parameters under study.

The statistic approach was a response surface design specifically the Central Composite in order to perform an optimization process. A previous study allowed to established the LG-MgO/MKP/ratio in 60/40 in a weight basis [36]. The total quantity of solid (S) is the sum of both MKP and LG-MgO. The ranges of the factors were selected according to the best of our knowledge in the topic of sust-MPC [38]. The two factors chosen for analysis were the water-to-solid ratio (W/S) and the percentage of boric acid (HB) added, where 0.24/0.32 and 0.44%/2.56% were the lowest/highest level, respectively. The percentage of HB refers to the weight of the solid mixture of MKP and LG-MgO, and is considered as an extra addition to the mortar formulations. The experimental plan was randomized in order to minimize systematic and accumulative errors on the results. The formulations under study are described in Table 1.

The analysis of DoE results is based on the analysis of variance (ANOVA) [44]. In this case, *p*-values have been used to interpret the obtained results. The *p*-value indicates whether the factor has a significant contribution to the model, represents the smallest level of significance that would lead to rejection of the null-hypothesis (i.e. there is no effect of the controllable factor on the response under investigation) while this hypothesis is true. A *p*-value lower than the level of significance ($\alpha = 0.05$) indicates significant contribution of the factor with a 95% of confidence. In other words, if a *p*-value in a test for the significance of a certain factor is smaller than 0.05, this factor is considered statistically significant at $\alpha = 0.05$ level of significance.

The F-value is defined as the ratio of the Model SS / Residual SS (Model SS and residual SS referred to the regression and error sum of squares, respectively). Large F-values indicate significant contribution while small values denote that the variance could be affected by noise.

2.3 Sust-MPC mortars formulation and preparation

The sust-MPC formulations were prepared by mixing the different solid reagents in a weight basis prior adding the kneading water. As aforementioned, formulations with a weight ratio of 60/40 of LG-MgO and MKP were considered and different amounts of HB and water (W/S) were added in order to determine an optimum proportion, as it is summarized in Table 1.

The mixing procedure was conducted as follows: MKP, LG-MgO and boric acid were weighed, respectively, and putted into a jar and carefully mixed in a dry state by hand operation using a spoon for 2 minutes. Afterwards, the kneading water was added and the mixing was conducted by a commonly planetary mortar mixer during 120 seconds at slow speed and 60 seconds at fast speed.

The resulting sust-MPC fresh mixture was cast in wood moulds with dimensions of 150×150×50 mm for characterization. Every formulation was vibrated for 3 seconds in order to remove the excess of entrapped air by means of a vibration table. Specimens were left in their moulds for 24 h in a curing chamber at a constant temperature of 20±2 ºC and a relative humidity of 95%. After demoulding, the specimens were left for further curing in the same conditions for up to 14 days. Then, each specimen was dried out using a desiccator with silica gel at room temperature (20±2 °C) during 14 days and the silica gel was removed when necessary. Thus, this unforced dried process carried out for all specimens was regarded to have no influence over the changes of porosity and the related thermal conductivity.

2.4 Testing procedures

The description of the testing and the specifications of the specimens are described below. Before the test procedure all the specimens were accurately weighted and

measured. All the experiments were carried out at 28 days (14 days of curing and 14 days of drying).

2.4.1 Thermal conductivity (*K*)

Thermal conductivity (*K*) was measured by using a Quickline-30 equipment. The equipment uses the principle of the transient heat line method instead of steady-state method [46]. The tests were conducted per triplicate for each specimen (150x150x50 mm) at room temperature (20±2 °C).

2.4.2 Determination of MOE (dynamic elasticity modulus of elasticity)

After the thermal conductivity test, the same specimens were used for determining the MOE following the standard UNE-EN 12504-4 [47], in which ultrasonic impulse velocity is used. The test consists in measuring the velocity at which the ultrasonic impulses propagate through the sample. A transmitting and receiving device of ultrasound C368 made by Matest (55 kHz transceiver sensors) was used for testing the same specimens from the first test. The time needed for the ultrasonic pulse to go through the test sample in the 50 mm direction was measured.

The results from the measurements were obtained by assuming that the expressions used in the estimation of the Young's modulus are valid in both isotropic and homogeneous media although sust-MPC mortars do not strictly comply with this condition.

2.4.3 Apparent density and open porosity

Porosity is key parameter for a building material because of its influence on durability and mechanical properties, among others. As it was aforementioned, MPC porosity is related with water release during the exothermic setting reaction. Therefore, the porosity accessible (open porosity) to water was measured. This is of great importance, as it is considered a significant factor for further studies concerning phase change materials

(PCM) impregnation of sust-MPC for TES. Open porosity and apparent density were determined according to the standard UNE-EN 1015-1 based on the Archimedes Principle.

3. Results and discussion

The response surface methodology (RSM) was successful for finding different optimal combination of MOE, *K*, apparent density and open porosity for sust-MPC formulation. A proper relationship between HB and W/S would improve the responses under study (MOE, *K*, apparent density and porosity) because RSM is a powerful tool in optimizing various responses. In every case the models obtained were statistically significant with lower *p*-values and small probabilities of being originated by noise. The DoE formulations under study are shown in Table 1, along with the experimental and predicted values of each response. Using Design Expert® software, the predicted values of each response were fitted by ignoring the cubic aliased models. Therefore, the statistical models were developed by making multiple analysis with the help of the experimental values determined.

In the case of thermal conductivity the best model fitting the experimental data was the reduced quadratic type, showing low standard deviation and high R squared statistics value (R^2): 0.05 and 0.87, respectively. For MOE, the reduced quadratic model revealed the best fitting of the experimental data with standard deviation and R^2 of 1.93 and 0.88, respectively. For apparent density, the model was fitted to a reduced quadratic model showing a R^2 of 0.89 and a standard deviation of 21.09. For open porosity, several statistical models were generated for fitting. Among these models, linear model was found to fit the data in the best manner instead of the quadratic types. In this case, R^2 of 0.80 and standard deviation of 1.67 were determined.

Additionally, the ANOVA parameters of the predicted response surface models are presented in Tables 2-5. The tables show the model terms that are statistically significant with *p*-value less than 0.05. However, it should be emphasized that the *p*-value of W/S in Table 2 is higher than 0.05 with a value of 0.0984. However, it is possible to consider this term because of the fit and only the values greater than 0.1000 indicate that the model terms are not significant.

Accordingly with the exposed, it can be stated that presented statistical models will be useful and appropriate to estimate the following properties in sust-MPC formulations.

3.1 Thermal conductivity (*K*)

Table 2 summarizes ANOVA results of thermal conductivity. As it is shown, a significant (*p*-value = 0.0014) statistical quadratic model is obtained. The factors under study (HB and W/S ratio) had a significant effect over the response. Figure 1 shows the thermal conductivity surface plot obtained. According to the results, an increase of boric acid or water led to a diminution of thermal conductivity. When both factors (W/S ratio and HB) are increased their combined effect is found to be lower than the expected from the sum of each one separately. Hence, it can be concluded that there is a significant negative interaction between these two factors (*p*-value = 0.0196, see Table 2) which explains this behaviour. The presence of water in the composites aided a better thermal insulation performance. In this case HB had higher effects on conductivity when water (or W/S ratio) is increased. With lower water amounts the effect of HB on the response is also lower.

All the results derived from the modification of any of the controllable variables can be translated into a predictive mathematical model. This model can quantitatively predict the response within the operating range of controllable variables. It can also give some

suitable formulations when a certain response is required. The model only incorporates the factors and interactions that are considered statistically significant. In this case a quadratic model describes the system. For the thermal conductivity (*K*) results, the model can be written according to the following equation:

$$K\left(\frac{W}{mK}\right) = -2.45 + 0.38HB + 24.95\left(\frac{W}{S}\right) - 1.66\left(\left(\frac{W}{S}\right)\cdot HB\right) - 41.54\left(\frac{W}{S}\right)^2 \quad (1)$$

3.2 MOE

Table 3 presents the ANOVA results for the MOE response. A significant (*p*-value=0.0002) statistically quadratic model is obtained for describing it. Both parameters under study affected significantly the response, resulting in a diminution of MOE when water and HB are separately increased in the formulations. There is not a significant interaction between the factors that affect the results, as it is shown in Table 3.

This behavior is depicted in Figure 2 and the mathematical model is described as follows:

$$MOE\ (GPa) = -23.33 - 2.79HB + 501.53\left(\frac{W}{S}\right) - 1077.55\left(\frac{W}{S}\right)^2 \quad (2)$$

As it is reported elsewhere, the addition of boric acid increases the setting time of the formulations [36]. Hence, during the setting time reaction there is a potential release of water that might lead to an increase of the open porosity. Therefore, MOE decreases as the W/S ratio increases, which might lead to a more porous formulation. In addition, MOE decreases as HB addition increases because water is released during longer periods of time. In other words, both factors lead to a more porous material and this is related with a lower MOE, as it is depicted in blue (Fig. 2, on-line version).

3.3 Apparent density and open porosity

Significant statistical models are obtained for apparent density and open porosity results, with the corresponding p-values (0.0001 -Table 4- and 0.0003 -Table 5- respectively). Figure 3 depicts the surface plot of apparent density and Figure 4 shows the surface plot of open porosity. In addition, equations 3 and 4 describe the mathematical model for each figure, respectively.

$$Apparent\ density\ (kg \cdot m^{-3}) = +1015.51 - 34.55HB + 8779.42\left(\frac{W}{S}\right) - 17408.87(W/S)^2 \quad (3)$$

$$Open\ porosity\ (\%) = -13.36 + 1.64HB + 77.92(W/S) \quad (4)$$

As it is shown in Figure 3 and mathematically described in Equation 3 there is no interaction between both factors in the range under study for the apparent density results. As expected, these results are in accordance to those obtained for the MOE results, where both factors had a significant effect in the response and had no mutual interaction. Then, an increase of HB percentage and W/S ratio separately decreases the apparent density in the range under study. Hence, this behavior can be explained in the same manner of the above mentioned MOE results.

Concerning the open porosity results (Fig 4 and Eq 4), no interaction between both factors was obtained. Moreover, both factors affected separately the response and the W/S ratio showed a higher effect than the HB percentage in the range of study. This could be explained due to the fact the total amount of water is higher as the W/S ratio is increased, resulting in a higher release of water. This fact could explain the higher open porosity obtained experimentally for the dosages with higher W/S ratios, such as RUN 1, RUN 4 and RUN 13 (see Table 1, experimental values of open porosity).

4. Optimization and validation process

On the basis of the statistical analysis presented above, a numerical optimization was performed in order to obtain the optimal composition of sust-MPC. The basic concept of optimization entails a compromise between values. The present research was focused on the development of sust-MPC with the lowest thermal conductivity. Therefore, the optimizations were assessed with the minimum thermal conductivity as reported in Table 6 for each criterion goal (CG). Thus, it was proposed to obtain the maximum and minimum open porosity and relate both extreme values to thermal conductivity, obtaining criterion goal 1 (CG1 – maximum porosity) and criterion goal 2 (CG2 – minimum porosity), respectively. These selections were made because the main purpose of this paper was to obtain a sust-MPC with a minimum thermal conductivity and desirable open porosity. This could be the starting point for further studies, i.e. sust-MPC impregnation with PCM in TES applications. Moreover, the maximum MOE could be also determined for improving the mechanical behavior if the material application requires it (criterion goal 3 - CG3- of Table 6). It is also possible to further enhance the mechanical behavior by increasing the apparent density, as it is included in criterion goal 4 (CG4) for maximum apparent density and minimum thermal conductivity.

Summarizing the abovementioned, the goals for each response are shown in Table 6, where lower and upper limits as well as the importance for each factor and response are included. The factors and responses under study were fitted in the range, maximized or minimized depending on the CG. It should be remarked that a scale of importance is included in the CG assessment: 3 for the cases where constrains fit the range and 5 when constrains were maximized or minimized.

Taking into account the CGs, a list of optimal mixture solutions was deduced, as it is shown in Table 7. Notice that two solutions were reached from CG1, CG2 and CG4 (Solutions 1 and 2; Solutions 3 and 4, and Solutions 6 and 7, respectively, Table 7) instead of CG3, where only one solution was obtained (Solution 5, Table 7). However, solutions 3, 5 and 6 were the same. On this manner, it can be just considered five potential solutions: solution 1, 2, 3, 4 and 7, for example. Figure 5 shows the contour diagram desirability for CG1. It is clearly shown the effect of HB and W/S on the desirability, where the dosages with higher values of each factor depicted the best desirability. Thus, it is possible to obtain less desirability by varying the dosages in case that it would be necessary, as an example: it can be reduced the cost by reducing HB content.

The model was validated using the optimal mixture solutions presented in Table 7. Nevertheless, solutions 2, 4 and 7 were the only dosages taken under consideration because solutions 1, 3, 5 and 6 corresponded to run 1 and run 2 from Table 1. Therefore, just the new optimal mixture solutions were prepared and the responses were determined following the same procedure explained in sections 2.3. and 2.4. Consequently, Table 8 shows experimental results of the 3 new formulations (solutions 2, 4 and 7) and those extracted from the experimental part presented in Table 1 (Run 1 and 2 for solutions 1, 3, 5 and 6). Table 8 also shows predicted values and standard deviation for each mixture and response. MOE experimental response of solution 1 was the unique that was not in accordance with predicted value range expected by the model. However, it is possible to affirm that the experimental values were in accordance with those predicted by the model. In other words, the validation demonstrates that the degree of fitting of the selected model is good and useful to further prediction of the responses.

Hence, the equations can be used to describe the relationship between open porosity and thermal conductivity as a function of W/S ratio and HB content. Figure 6 depicts equations 1 and 4 for the range under study (i.e.: HB content (0.44 to 2.56), W/S ratio (0.24 to 0.32) using a response surface graph. Moving towards the right of the surface the W/S ratio is increased, and from the top to the bottom of the surface the HB content is also increased, as it is shown by arrows in the graph. There was a downward trend in thermal conductivity as open porosity was increased. Moreover, a wide range of open porosity values are allowed above K = 1.1 $W \cdot m^{-1} \cdot K^{-1}$ while just a restricted open porosity values are allowed below this value of thermal conductivity. Hence, it can be concluded that the dependency of thermal conductivity with open porosity is more important at low values of thermal conductivity. By this manner, thermal conductivity is low when open porosity presents low values and becomes high when open porosity is correlated to both values.

5. Conclusions

A statistical method was employed in order to predict the effects of variables on the final properties of sust-MPC. By this manner, a model that explains the overall behaviour of the system could be established. This set of models allows not only to estimate the response of each formulation but also to optimize the whole system in order to obtain a compromise between the factors constraints and the responses. The application of the design of experiments methodology is of great aid for understanding the interaction between different variables that otherwise could not be studied using a single variable method. Accordingly, the model allows to control the porosity and, therefore, the thermal conductivity of sust-MPC by means of mixture dosage. The proper addition of HB and water (W/S ratio) leads to an increase of open porosity. The

determined properties: apparent density, elastic modulus and thermal conductivity are related with open porosity. Hence, the measurement of the MOE could be an easy and fast method to predict the open porosity and thermal conductivity for sust-MPC.

The present work demonstrated that it is possible to control the porosity in order to diminish thermal conductivity. Besides, this work will be the starting point for further modifications of sust-MPC for TES application, which is in accordance with the sustainability criteria of the nowadays research. The authors considered that this study could be a useful approach for researchers and technicians in the field of isolating building materials.

6. Acknowledgements

The authors would like to thank Magnesitas Navarras, S.A. for supporting and financing this research project.

7. Bibliography

[1] S.J. Pantazopoulou, R.H. Mills, Microstructural aspects of the mechanical response of plain concrete, ACI Mater. J. 92 (1995) 605–616.

[2] M. Yudenfreund, K.M. Hanna, J. Skalny, I. Older, S. Brunauer, Hardened Portland cement pastes of low porosity V. Compressive strength, Cem. Concr. Res. 2 (1972) 731–743.

[3] X. Chen, S. Wu, J. Zhou, Influence of porosity on compressive and tensile strength of cement mortar, Constr. Build. Mater. 40 (2013) 869–874.

[4] X. Zhou, F. Zheng, H. Li, C. Lu, An environment-friendly thermal insulation material from cotton stalk fibers, Energy Build. 42 (2010) 1070–1074.

[5] J. Olmeda, M.I. Sánchez de Rojas, M. Frías, S. Donatello, C.R. Cheeseman, Effect of petroleum (pet) coke addition on the density and thermal conductivity of cement pastes and mortars, Fuel. 107 (2013) 138–146.

[6] V. Ducman, A. Mladenovič, J.S. Šuput, Lightweight aggregate based on waste glass and its alkali–silica reactivity, Cem. Concr. Res. 32 (2002) 223–226.

[7] A. Benazzouk, O. Douzane, K. Mezreb, B. Laidoudi, M. Quéneudec, Thermal conductivity of cement composites containing rubber waste particles: Experimental study and modelling, Constr. Build. Mater. 22 (2008) 573–579.

[8] A. Bouguerra, A. Ledhem, F. De Barquin, R.M. Dheilly, M. Quéneudec, Effect of microstructure on the mechanical and thermal properties of lightweight concrete prepared from clay, cement, and wood aggregates, Cem. Concr. Res. 28 (1998) 1179–1190.

[9] E. Kamseu, B. Nait-Ali, M.C. Bignozzi, C. Leonelli, S. Rossignol, D.S. Smith, Bulk composition and microstructure dependence of effective thermal conductivity of porous inorganic polymer cements, J. Eur. Ceram. Soc. 32 (2012) 1593–1603.

[10] W.N. dos Santos, Effect of moisture and porosity on the thermal properties of a conventional refractory concrete, J. Eur. Ceram. Soc. 23 (2003) 745–755.

[11] F.I.P.C. on Lightweight Concrete, Principles of Thermal Insulation Wih Respect to Lightweight Concrete, FIP, 1978.

[12] P. Morabito, Measurement of the thermal properties of different concretes, High Temp. - High Press. 21 (1989) 51–59.

[13] R.W. Steiger, M.K. Hurd, LIGHTWEIGHT INSULATING CONCRETE FOR FLOORS AND ROOF DECKS., Concr. Constr. - World Concr. 23 (1978) 411–413, 415, 420, 422.

[14] İ. Örüng, TARIMSAL YAPILARDA ÖĞÜTÜLMÜŞ HAFİF AGREGANIN KULLANILABİLME OLANAKLARI ÜZERİNE BİR ARAŞTIRMA, J. Fac. Agric. 26 (1995).

[15] R.S. Graves, D.C. Wysocki, Insulation Materials: Testing and Applications, American Society for Testing and Materials, 1991.

[16] X. Fu, D.D.L. Chung, Effects of silica fume, latex, methylcellulose, and carbon fibers on the thermal conductivity and specific heat of cement paste, Cem. Concr. Res. 27 (1997) 1799–1804.

[17] D.M. ROY, New Strong Cement Materials: Chemically Bonded Ceramics, Science (80-.). 235 (1987) 651–658.

[18] A.S. Wagh, R. Strain, S.Y. Jeong, D. Reed, T. Krause, D. Singh, Stabilization of Rocky Flats Pu-contaminated ash within chemically bonded phosphate ceramics., J. Nucl. Mater. 265 (1999) 295–307.

[19] I. Buj, J. Torras, M. Rovira, J. de Pablo, Leaching behaviour of magnesium

phosphate cements containing high quantities of heavy metals., J. Hazard. Mater. 175 (2010) 789–794.
[20] P. Randall, S. Chattopadhyay, Advances in encapsulation technologies for the management of mercury-contaminated hazardous wastes ☪, 114 (2004) 211–223.
[21] A.S. Wagh, S.Y. Jeong, Chemically bonded phosphate ceramics: I, A dissolution model of formation., J. Am. Ceram. Soc. 86 (2003) 1838–1844.
[22] A.S. Wagh, Chapter 3 - Raw Materials, in: A.S.B.T.-C.B.P.C. Wagh (Ed.), Elsevier, Oxford, 2004: pp. 29–41.
[23] S. Graeser, W. Postl, H. Bojar, P. Berlepsch, T. Armbruster, Struvite- (K), KMgPO 4 · 6H 2 O , the potassium equivalent of struvite – a new mineral, (2008) 629–633.
[24] Z. Ding, Z.J. Li, Effect of aggregates and water contents on the properties of magnesium phospho-silicate cement, Cem. Concr. Compos. 27 (2005) 11–18.
[25] Z. Ding, B. Dong, F. Xing, N. Han, Z. Li, Cementing mechanism of potassium phosphate based magnesium phosphate cement, Ceram. Int. 38 (2012) 6281–6288.
[26] Y. Li, J. Sun, B. Chen, Experimental study of magnesia and M/P ratio influencing properties of magnesium phosphate cement, Constr. Build. Mater. 65 (2014) 177–183.
[27] H. Ma, B. Xu, Z. Li, Magnesium potassium phosphate cement paste: Degree of reaction, porosity and pore structure, Cem. Concr. Res. 65 (2014) 96–104.
[28] J. Li, G. Xu, Y. Chen, G. Liu, Multiple scaling investigation of magnesium phosphate cement modified by emulsified asphalt for rapid repair of asphalt mixture pavement, Constr. Build. Mater. 69 (2014) 346–350.
[29] J. Li, W. Zhang, Y. Cao, Laboratory evaluation of magnesium phosphate cement paste and mortar for rapid repair of cement concrete pavement, Constr. Build. Mater. 58 (2014) 122–128.
[30] Y. Tan, H. Yu, Y. Li, C. Wu, J. Dong, J. Wen, Magnesium potassium phosphate cement prepared by the byproduct of magnesium oxide after producing Li2CO3 from salt lakes, Ceram. Int. 40 (2014) 13543–13551.
[31] Y. Li, B. Chen, Factors that affect the properties of magnesium phosphate cement, Constr. Build. Mater. 47 (2013) 977–983.
[32] C. Shi, J. Yang, N. Yang, Y. Chang, Effect of waterglass on water stability of potassium magnesium phosphate cement paste, Cem. Concr. Compos. 53 (2014) 83–87.
[33] S. Manso, G. Mestres, M.P. Ginebra, N. De Belie, I. Segura, A. Aguado, Development of a low pH cementitious material to enlarge bioreceptivity, Constr. Build. Mater. 54 (2014) 485–495.
[34] H. Ma, B. Xu, J. Liu, H. Pei, Z. Li, Effects of water content, magnesia-to-phosphate molar ratio and ageon pore structure, strength and permeability of magnesium potassium phosphate cement paste, Mater. Des. 64 (2014) 497–502.
[35] M. Morales, J. Formosa, E. Xuriguera, M. Niubó, M. Segarra, J.M. Chimenos, Elastic modulus of a chemically bonded phosphate ceramic formulated with low-grade magnesium oxide determined by Nanoindentation, Ceram. Int. 41 (2015) 12137–12146.
[36] J. Formosa, J.M. Chimenos, A.M. Lacasta, M. Niubó, Interaction between low-grade magnesium oxide and boric acid in chemically bonded phosphate ceramics formulation, Ceram. Int. 38 (2012) 2483–2493.
[37] R. del Valle-Zermeño, J.E. Aubert, A. Laborel-Préneron, J. Formosa, J.M. Chimenos, Preliminary study of the mechanical and hygrothermal properties of

hemp-magnesium phosphate cements, Constr. Build. Mater. 105 (2016) 62–68.
[38] J. Formosa, A.M. Lacasta, A. Navarro, R. del Valle-Zermeño, M. Niubó, J.R. Rosell, et al., Magnesium Phosphate Cements formulated with a low-grade MgO by-product: Physico-mechanical and durability aspects, Constr. Build. Mater. 91 (2015) 150–157.
[39] J. Formosa, M. A. Aranda, J.M. Chimenos, J.R. Rosell, a. I. Fernández, O. Ginés, Cementos químicos formulados con subproductos de óxido de magnesio, Bol. La Soc. Esp. Ceram. Y Vidr. 47 (2008) 293–297.
[40] A.J. Wang, J. Zhang, J.M. Li, A.B. Ma, L.T. Liu, Effect of liquid-to-solid ratios on the properties of magnesium phosphate chemically bonded ceramics, Mater. Sci. Eng. C. 33 (2013) 2508–2512.
[41] R.M. Novais, M.P. Seabra, J.A. Labrincha, Ceramic tiles with controlled porosity and low thermal conductivity by using pore-forming agents, Ceram. Int. 40 (2014) 11637–11648.
[42] E. Rambaldi, F. Prete, M.C. Bignozzi, Acoustic and thermal performances of ceramic tiles and tiling systems, Ceram. Int. 41 (2015) 7252–7260.
[43] I. State-Ease, Design-Expert® Software Version 7.0.
[44] D.C. Montgomery, Design and Analysis of Experiments, 6th Edition Set, John Wiley & Sons, Limited, 2007.
[45] M. Niubó, A.I. Fernández, L. Haurie, X.G. Capdevila, J.M. Chimenos, J.I. Velasco, Influence of the Electric Arc Furnace Dust in the physical and mechanical properties of EVA–polyethylene–butene blends, Mater. Sci. Eng. A. 528 (2011) 4437–4444.
[46] A.H.-C. Shin, U. Kodide, Thermal conductivity of ternary mixtures for concrete pavements, Cem. Concr. Compos. 34 (2012) 575–582.
[47] UNE-EN, UNE-EN 12504-4:2006 Testing concrete - Part 4: Determination of ultrasonic pulse velocity, 2006.

Figure Caption

Figure 1. Surface plot of the thermal conductivity as a function of W/S ratio and HB.

Figure 2. Surface plot of the modulus of elasticity as a function of W/S ratio and HB.

Figure 3. Surface plot of the apparent density as a function of W/S ratio and HB.

Figure 4. Surface plot of the open porosity as a function of W/S ratio and HB.

Figure 5. Contour diagram desirability for CG1 (minimize *K* and maximize open porosity) as a function of W/S ratio and HB.

Figure 6. Thermal conductivity versus open porosity by using model equations.

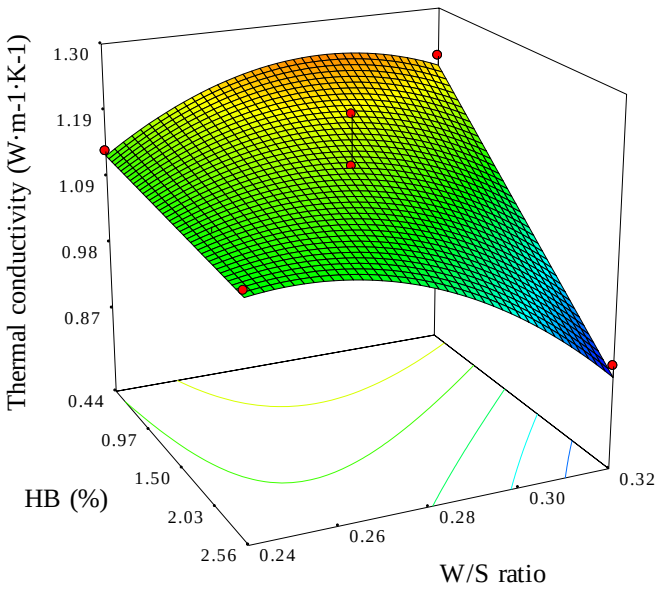

Fig. 1
(M. Niubó et al.)

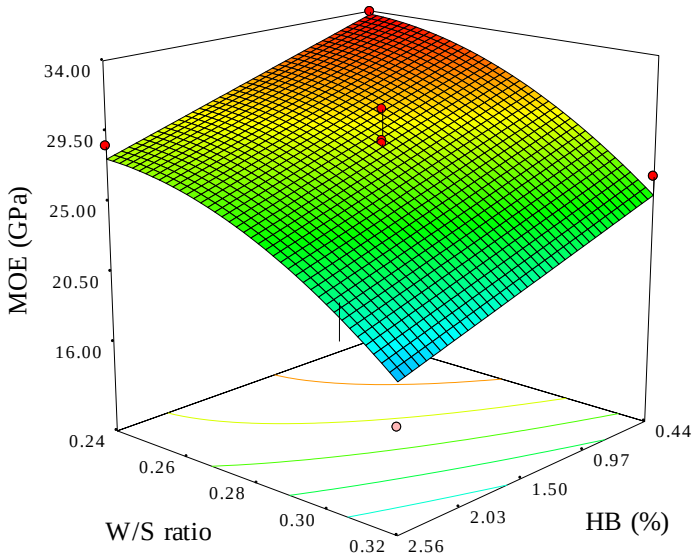

Fig. 2
(M. Niubó et al.)

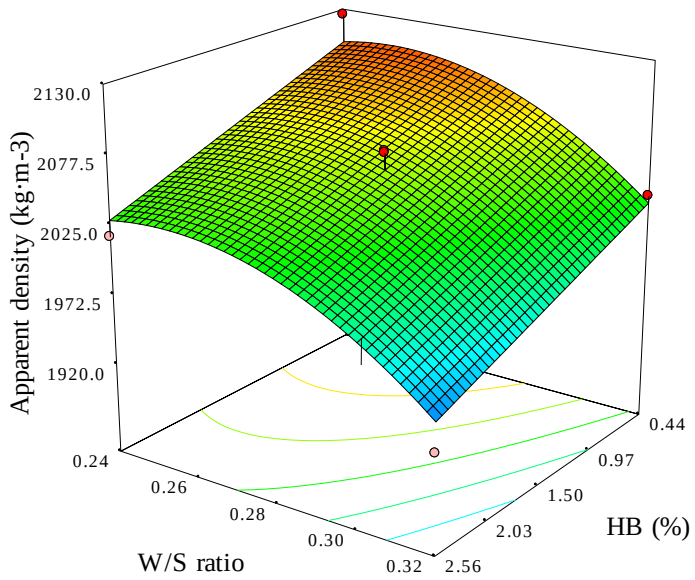

Fig. 3
(M. Niubó et al.)

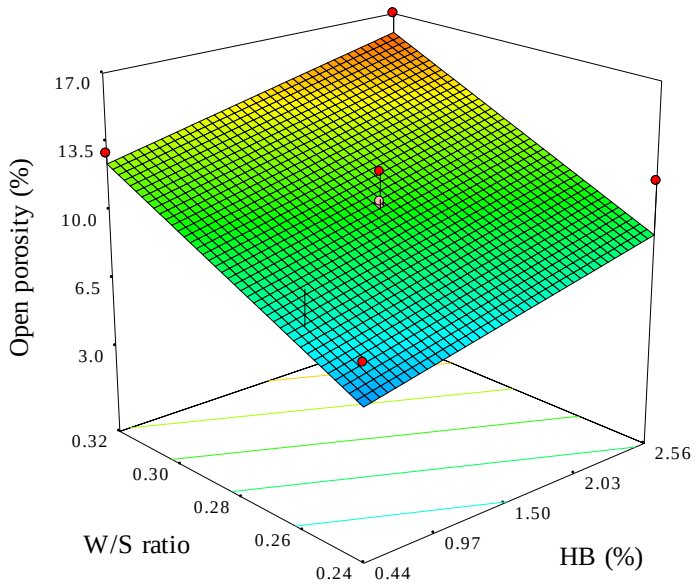

Fig 4.
(M. Niubó et al.)

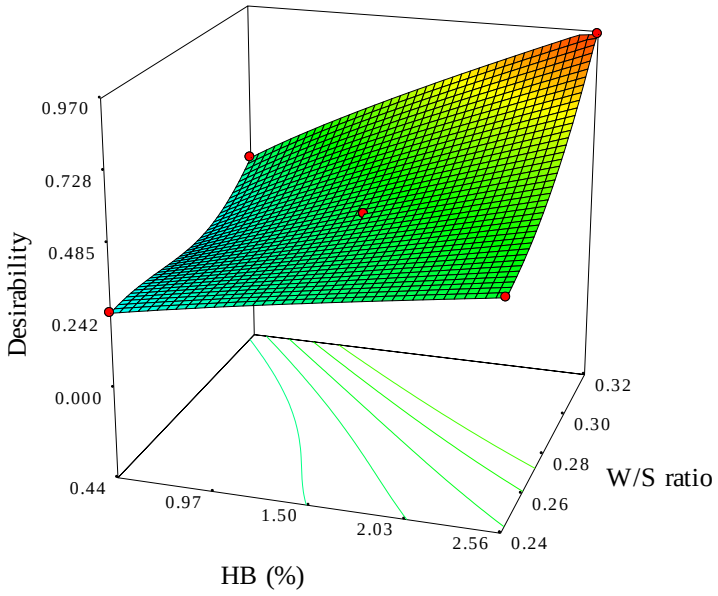

Fig 5.
(M. Niubó et al.)

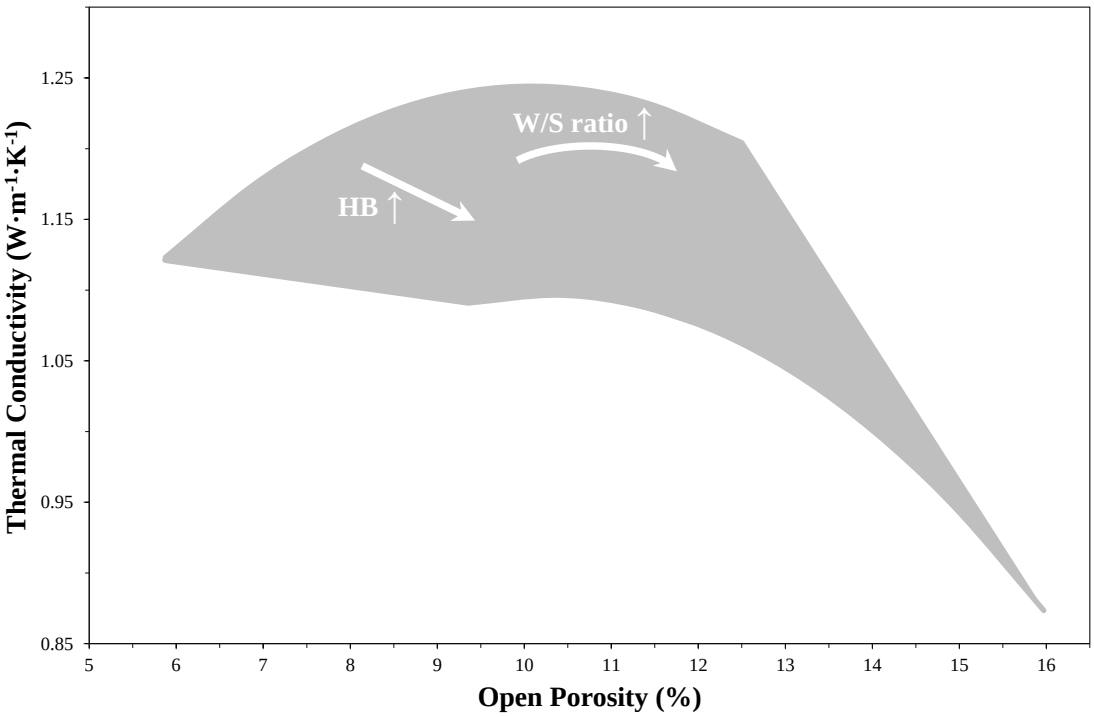

Fig 6.
(M. Niubó et al.)

Table 1. Formulations under study and characterization results

Run	Factors		MOE (GPa)		*K* ($W \cdot m^{-1} \cdot K^{-1}$)		Apparent density ($kg \cdot m^{-3}$)		Porosity (%)	
	HB (%)	W/S	Experimental value	Predicted value	Experimental value	Predicted value	Experimental value	Predicted value	Experimental value	Predicted value
1	2.56	0.32	16.50	19.22	0.89	0.87	1925.2	1948.0	17.0	16.0
2	0.44	0.24	33.92	33.78	1.13	1.12	2125.5	2103.5	7.9	5.9
3	1.50	0.28	24.90	28.44	1.06	1.15	2031.5	2057.1	12.3	10.9
4	1.50	0.34	19.47	18.44	0.93	0.95	1947.7	1936.2	15.5	15.6
5	1.50	0.22	29.95	30.67	1.04	1.02	2045.1	2052.6	3.8	6.3
6	1.50	0.28	27.74	28.44	1.08	1.15	2071.5	2057.1	10.6	10.9
7	2.56	0.24	28.65	27.86	1.10	1.09	2017.7	2030.2	12.1	9.4
8	1.50	0.28	28.60	28.44	1.15	1.15	2070.0	2057.1	10.0	10.9
9	0.00	0.28	32.30	32.62	1.30	1.28	2074.8	2108.9	7.2	8.5
10	1.50	0.28	28.80	28.44	1.15	1.15	2070.0	2057.1	10.8	10.9
11	1.50	0.28	30.80	28.44	1.23	1.15	2070.1	2057.1	10.5	10.9
12	3.00	0.28	26.23	24.25	1.04	1.05	2015.5	2005.3	11.3	13.4
13	0.44	0.32	26.31	25.13	1.22	1.20	2026.7	2021.2	13.0	12.5

Table 2. ANOVA results for thermal conductivity (*K*) response surface reduced quadratic model

Source	Sum of squares	df	Mean Square	F Value	*p*-value Prob > F
Model	0.137157	4	0.034289	12.99602	0.0014
HB	0.066011	1	0.066011	25.01888	0.0011
W/S	0.00923	1	0.00923	3.498278	0.0984
HB*(W/S)	0.02235	1	0.02235	8.471012	0.0196
$(W/S)^2$	0.039566	1	0.039566	14.99589	0.0047
Residual	0.021108	8	0.002638		
Lack of Fit	0.002988	4	0.000747	0.164874	0.9456
Pure Error	0.01812	4	0.00453		
Cor Total	0.158264	12			

Table 3. ANOVA results for MOE response surface reduced quadratic model

Source	Sum of squares	df	Mean Square	F Value	*p*-value Prob > F
Model	246.142218	3	82.047406	21.917440	0.0002
HB	69.999686	1	69.999686	18.699115	0.0019
W/S	149.519209	1	149.519209	39.941278	0.0001
$(W/S)^2$	26.623324	1	26.623324	7.111926	0.0258
Residual	33.691282	9	3.743476		
Lack of Fit	15.323671	5	3.064734	0.667421	0.6703
Pure Error	18.367611	4	4.591903		
Cor Total	279.833500	12			

Table 4. ANOVA results for apparent density response surface reduced quadratic model

Source	Sum of squares	df	Mean Square	F Value	*p*-value Prob > F
Model	31227.48342	3	10409.16114	23.39489186	0.0001
HB	10741.95548	1	10741.95548	24.1428568	0.0008
W/S	13536.39255	1	13536.39255	30.42343525	0.0004
$(W/S)^2$	6949.135389	1	6949.135389	15.61838353	0.0033
Residual	4004.397662	9	444.9330735		
Lack of Fit	2794.10967	5	558.8219341	1.846905655	0.2860
Pure Error	1210.287991	4	302.5719979		
Cor Total	35231.88108	12			

Table 5. ANOVA results for porosity response surface linear model

Source	Sum of squares	df	Mean Square	F Value	*p*-value Prob > F
Model	111.7169	2	55.85846	20.13287	0.0003
HB	24.28444	1	24.28444	8.752757	0.0143
W/S	87.43248	1	87.43248	31.51299	0.0002
Residual	27.74491	10	2.774491		
Lack of Fit	24.73291	6	4.122151	5.474304	0.0609
Pure Error	3.012	4	0.753		
Cor Total	139.4618	12			

Table 6. Optimization criterions used in this study

Constraints Name	*CG1*	*CG2*	*CG3*	*CG4*	Limits		Importance
					Lower	Upper	
HB	is in range	is in range	is in range	is in range	0.44	2.56	3
W/S	is in range	is in range	is in range	is in range	0.24	0.32	3
MOE (GPa)	is in range	is in range	maximize	is in range	16.50	33.92	3 or 5
K ($W \cdot m^{-1} \cdot K^{-1}$)	minimize	minimize	minimize	minimize	0.89	1.30	5
Apparent density ($kg \cdot m^{-3)}$	is in range	is in range	is in range	maximize	1925.19	2125.46	3 or 5
Porosity (%)	maximize	minimize	is in range	is in range	3.8	17.0	3 or 5

Table 7. Optimal mixture solutions based on the criterion goals

Solutions	HB (%)	W/S	Desirability
CG1			
1	2.56	0.32	0.96012
2	2.46	0.32	0.95334
CG2			
3	0.44	0.24	0.60453
4	1.65	0.24	0.57554
CG3			
5	0.44	0.24	0.65505
CG4			
6	0.44	0.24	0.62065
7	2.52	0.28	0.53176

Table 8. Validation of optimal mixture solutions based on the criterion goals

Solutions	MOE (GPa)		K ($W \cdot m^{-1} \cdot K^{-1}$)		Apparent density ($kg \cdot m^{-3}$)		Porosity (%)	
	Experimental	Predicted	Experimental	Predicted	Experimental	Predicted	Experimental	Predicted
CG1								
1	16.50	19.22 (16.63-21.80)	0.89	0.87 (0.78-0.97)	1925.2	1948.0 (1919.8-1976.1)	17.0	16.0 (13.8-18.1)
2	17.05	19.51 (17.01-22.00)	0.91	0.89 (0.80-0.98)	1962.3	1951.6 (1924.4-1978.8)	16.5	15.8 (13.8-17.8)
CG2								
3	33.92	33.78 (31.20-36.36)	1.13	1.12 (1.03-1.21)	2125.5	2103.5 (2075.4-2131.7)	7.9	5.9 (3.8-8.0)
4	29.89	30.40 (28.32-32.48)	1.11	1.10 (1.04-1.16)	2079.8	2061.7 (2039.0-2084.3)	7.1	7.9 (6.2-9.5)
CG3								
5	33.92	33.78 (31.20-36.36)	1.13	1.12 (1.03-1.21)	2125.5	2103.5 (2075.4-2131.7)	7.9	5.9 (3.8-8.0)
CG4								
6	33.92	33.78 (31.20-36.36)	1.13	1.12 (1.03-1.21)	2125.5	2103.5 (2075.4-2131.7)	7.9	5.9 (3.8-8.0)
7	25.89	25.44 (23.28-27.61)	1.03	1.06 (1.00-1.12)	2013.6	2020.5 (1996.8-2044-1)	12.5	12.7 (11.1-14.3)